Optical transitions in $Zn_{1-x}Co_xSe$ and $Zn_{1-x}Fe_xSe$: Strong concentration-dependent effective p-d exchange

Chee-Leung Mak, R. Sooryakumar, and M. M. Steiner
Department of Physics, The Ohio State University, Columbus, Ohio 43210

B. T. Jonker
Naval Research Laboratory, Washington, D.C. 20375

(Received 30 April 1993)

Results of photoluminescence (PL) and resonant Raman scattering from single crystalline epitaxial films of $Zn_{1-x}Co_xSe$ and $Zn_{1-x}Fe_xSe$ are presented. Samples with Co concentrations up to $x=0.1$ and Fe concentrations in the range $0<x<0.75$ were studied. For $x<0.03$ (Co) and $x<0.30$ (Fe) the optical emission associated with the $3d$ deep levels are observed as discrete transitions that broaden very rapidly and weaken as the doping further increases. It is proposed that the increase in concentration x leads to an increase in the exchange between low-lying crystal-field split d levels and band electrons, and thus to the changes in the photoluminescence. Concomitant with the onset of broadening of the PL, a continuum of Raman excitations extending from zero to about 4000 cm^{-1} is observed which is resonantly enhanced as the energy of the exciting radiation approaches the alloy band gap from below. The Raman-scattering features are discussed in terms of electronic scattering within the $3d$-ion band manifold located in the gap of the insulating host. The role of strong disorder and correlations on the electronic Raman excitations in these insulating structures are briefly addressed.

I. INTRODUCTION

Shallow donors in semiconductors is a topic that has been extensively studied. A classic example of such a system is phosphorous-doped silicon where the donor electron can be viewed as a hydrogenlike s electron with a Bohr radius, a^*, larger than several lattice spacings. In the low concentration limit when a^* is smaller than the near-neighbor donor separation, the optical absorption spectrum consists of sharp lines corresponding to excitations from the ground state to various bound excited states. As the donor density increases and the insulator to metal transition is approached, the isolated donor lines initially broaden asymmetrically and are subsequently washed out yielding a broad featureless absorption band.[1] In the metallic regime absorption is governed by donor clusters, and therefore the spectrum remains devoid of sharp density-of-state characteristics. The effects of increased doping are also manifested through other elementary excitations. For example, Raman excitations between valley-orbit split states rapidly broaden and a Raman continuum due to inter-valley fluctuations appears as the metallic state is approached.[2,3] This continuum eventually dominates the low-energy Raman spectrum well beyond the insulator-metal transition. Further, in the heavily doped material, the inter-conduction-band transitions interfere with the zone center optical phonon to produce Fano-type asymmetric phonon line shapes.[4] These diverse optical features are generally well understood in terms of an ideal paradigm of random hydrogenic atoms with one s electron per site.

Diluted magnetic semiconductors (DMS), which are typically solid solutions formed by alloying a nonmagnetic semiconductor compound with a $3d$ transition-metal ion, offer an interesting dimension to the study of substitutional dopants in semiconductors. They differ from the hydrogenic donors discussed above in the following important ways. (1) Since the $4s^2$ electrons of the magnetic ion contribute to bonding in the same fashion as the two outer s electrons of the group-II element, the crystal-field split manifold of d levels plays a major role in the optical and electronic properties of the DMS. (2) Unlike the large Bohr radii of hydrogenic donors, d orbitals are localized to a single site. Hence about three orders of magnitude larger doping than Si:P is required before interactions among substitutional ions become important. (3) The existence of large exchange interactions between band electrons and the $3d$ ion, the so-called s,p-d interaction, will lead to the d electrons being more extended. (4) As evidenced by the impurity spin moment, the $3d$ ions often have strong intra-ion Coulomb correlation. Thus correlations, together with the high spatial disorder introduced by the random substitution of $3d$ ions can lead to a continuum of *localized* electronic states. Hence in contrast to the shallow donor case, the insulator to metal transition will be inhibited even when impurity band formation occurs.

Work to date in these DMS systems has largely concentrated on Mn-doped II-VI semiconductors and the results are summarized in several reviews.[5,6] Signatures associated with electronic levels in Mn^{2+} have been identified up to about 70% mole fraction in $Cd_{1-x}Mn_xTe$,[7] and to lower Mn concentrations in $Zn_{1-x}Mn_xTe$,[8] $Zn_{1-x}Mn_xSe$,[9] and $Zn_{1-x}Mn_xS$.[10] Even at the highest Mn concentrations studied ($x\approx 0.70$), there is no evidence that the isolated atomiclike Mn^{2+}

levels in the II-VI lattice are modified through inter $3d$-ion interactions.

In this paper we report on photoluminescence and Raman studies that directly probe the $3d$-ion levels in $Zn_{1-x}Co_xSe$ and $Zn_{1-x}Fe_xSe$. The introduction of Fe and Co to the ZnSe lattice is a relatively recent advance,[11] and these systems are characterized by s,p-d and d-d exchange interactions that are significantly enhanced over those of their Mn counterparts.[12] It has been demonstrated[11] that up to 10% Co and 100% Fe can be incorporated into ZnSe. We find that these $3d$-ion concentrations, together with the magnified exchange interactions, allow the crossover from isolated deep levels to a continuum of hybridized d states. As x increases, intra-ion transitions within the crystal-field split $3d$ manifold broaden and weaken. Concomitant with the broadening of the optical transitions a featureless Raman continuum is observed which extends to about 0.5 eV due to intra-band excitations within the newly formed impurity band. While observation of such a Raman continuum is evidence of an impurity band, Hall measurements confirm that the materials remain insulting to the highest Co and Fe concentrations. We argue that strong correlations and disorder give rise to a distribution of electronic states required to form the Raman continuum while retaining the insulating nature of the samples.

In the next section we discuss the experimental details with the results of our measurements being presented in Sec. III. Section IV is devoted to a discussion of the photoluminescence and Raman-scattering results. The conclusions are presented in Sec. V.

II. EXPERIMENTAL DETAILS

The $Zn_{1-x}Co_xSe$ and $Zn_{1-x}Fe_xSe$ samples used in our study were single-crystal epilayers grown by molecular-beam epitaxy on (001) GaAs substrates. Details of the growth conditions have been published elsewhere.[13] The epilayer thickness ranged from 0.25 to 2.6 μm with $x \leq 0.094$ for Co, and $0 \leq 0.75$ for Fe. All films were oriented with the [001] direction (z axis) normal to the surface. The luminescence and Raman spectra were excited using the 457.9-, 476.5-, 488.0-, and 514.5-nm lines of an Ar^+-ion laser with about 100 mW incident power. The spectra were recorded in a backscattering geometry and analyzed with a Spex double-grating monochromator using standard single-channel photon-counting techniques. Hall measurements, utilizing standard four-terminal methods, were carried out at room temperature on all films to determine the carrier concentration. The epilayers were all found to be highly resistive with nominal macroscopic carrier concentrations well below 10^{14} cm^{-3}.

III. EXPERIMENTAL RESULTS

Figure 1 shows photoluminescence (PL) and Raman spectra at 10 K in the vicinity of the intra-Co ion transitions in $Zn_{1-x}Co_xSe$. In the absence of Co, i.e., nominally pure ZnSe, luminescence bands centered at 2.60 (Y), 2.57 (Y-LO), 2.53 (S_0), 2.50 (S_1), 2.24 (SA_1), 2.09(SA_2), and 1.92 eV (SA_3) are observed when excited at 457.9 nm. Since the excitation energy is less than the band gap, band-edge PL is not observed. With the addition of Co, this emission from ZnSe is quenched and three different luminescence bands labeled I, II, and III develop as x increases to 0.016. Luminescence I, with the strong zero-phonon line (ZPL) L at 2.361 eV is the most prominent feature at low Co concentrations. The structure on the

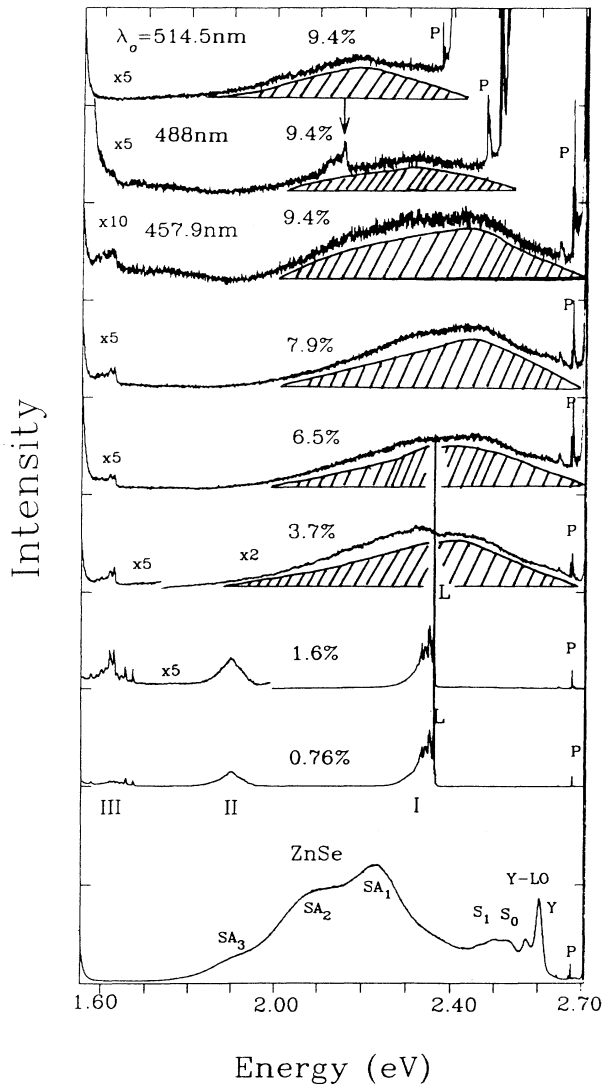

FIG. 1. Photoluminescence (PL) and Raman spectra at 10 K from ZnSe, and several $Zn_{1-x}Co_xSe$ films for x up to 0.094. All spectra, except the top two, were recorded with 457.9 nm excitation wavelength. Features labeled I, II, and III identify PL, with peak L being the strongest emission for the lower Co concentrations. The hatched regions for $x > 0.037$ highlight the continuum of Raman excitations, while the sharp peaks P are Raman phonons. The peak identified by the arrow in the 488.0-nm spectrum is impurity related. All spectra have been normalized to account for the different film thicknesses.

low-energy side of L has been shown,[14] for $x < 0.01$, to approximately replicate peaks in the phonon density-of-states of ZnSe. Two other PL transitions at 1.88 eV (luminescence II) and 1.62 eV (luminescence III) are also evident. Luminescence III is broad and underlies several sharp lines. The full width at half maximum (FWHM) of bands II and III (~ 60 meV) are much larger than that of peak L (0.37 meV).

As the Co concentration increases to 3.7%, PL I and II weaken drastically and are not evident beyond $x = 0.037$. While some emission associated with band III is similarly reduced, a few weak peaks of band III remain relatively sharp until $x \sim 0.09$. Concomitant with the suppression of the main PL bands at $x = 0.037$, a broad Raman peak centered at a frequency shift of ~ 2000 cm^{-1} emerges. This inelastic scattering is shown as hatched regions in Fig. 1. The Raman nature of this broad excitation is confirmed by its observation at 488.0 and 514.5 nm exciting radiation as shown in the top of Fig. 1. In addition to the PL bands I, II, and III, Fig. 1 shows peaks labeled P that are associated with Raman scattering from phonons.

Figure 2 shows the effect of different excitation wavelengths (λ_0) on the 10-K emission spectra of $Zn_{1-x}Co_xSe$ for $x = 0.016$. The PL features are strongest when excited at 457.9 nm. For 476.5-nm excitation, the sharp L transition in band I and band II are retained. Luminescence III changes dramatically upon exciting at 476.5 nm. Four absorption dips ($A_1 - A_4$) appear which become even more pronounced when λ_0 increases to 488.0 nm. Excitation at 514.5 and 488.0 nm yield similar spectra with the emission and absorption dips in the latter spectra being stronger. There is a rapid increase in emission below 1.6 eV as λ_0 increases towards 510 nm. As discussed below, this low-energy emission originates from the GaAs substrate and becomes more evident as the ZnCoSe epilayer becomes transparent to the incident radiation. The absorption dips ($A_1 - A_4$) in the vicinity of band III are directly related to the presence of this GaAs luminescence. In addition, a Raman peak that is clearly seen when excited at 488.0 nm (identified by arrows in Figs. 1 and 2) at a frequency shift of 3100 cm^{-1} is observed in the ZnSe film as well as in all Co-doped (and Fe-doped) sample. This peak is hence not intrinsic to the 3d dopants.

The polarized and depolarized components of the broad Raman peak in the $x = 0.094$ sample recorded at 10 K are shown in Fig. 3 for three different exciting wavelengths. x, y denote directions parallel to the cubic [100] and [010] directions. The primary feature is the broad Raman peak centered at 2000 cm^{-1}, where both $z(xx)\bar{z}$ and $z(xy)\bar{z}$ spectra have comparable intensities. Similar inelastic scattering features that steadily increase from $\omega \sim 0$ to frequency shifts ~ 2000 cm^{-1} are observed in all films with Co concentrations larger than about 3% (Fig. 1). The wavelength dependence, while confirming the Raman character of the continuum, also establishes its strong resonance enhancement as the energy of the exciting radiation approaches the alloy band gap from below.

Figure 4 shows PL and Raman spectra, excited at two different wavelengths, of $Zn_{1-x}Fe_xSe$ for Fe concentrations up to $Zn_{0.27}Fe_{0.73}Se$. Again the PL peaks from ZnSe are rapidly quenched with the addition of Fe and an impurity Raman peak at 3100 cm^{-1} is observed in all Fe-doped films. For $x \leq 0.22$, the main feature is a peak at ~ 1.89 eV with a FWHM ~ 70 meV. For $x \geq 0.22$, this PL broadens and the peak position shifts to 1.94 eV and FWHM ~ 150 meV at $x = 0.34$. As the Fe content further increases to $x \sim 0.73$, this emission weakens and continues to broaden. A broad Raman mode is observed beyond $x = 0.34$ that displays characteristics similar to the continuum observed in the Co-doped samples. These common characteristics include the location of the peak

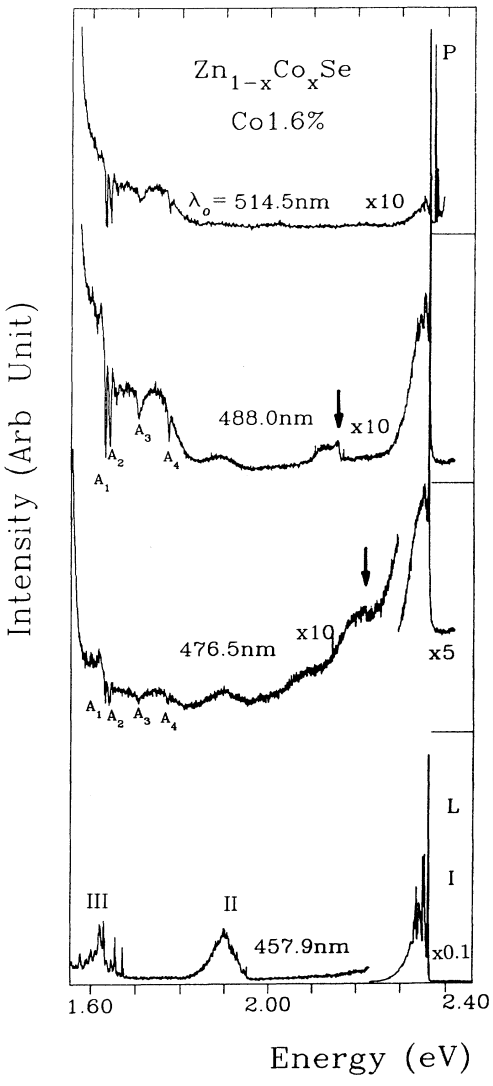

FIG. 2. Photoluminescence (PL) spectra at 10 K from $Zn_{1-x}Co_xSe$ ($x = 0.016$) for different excitation wavelengths. Features I, II, and III are PL associated with transitions within crystal-field split Co^{2+} manifold. A_1, A_2, A_3, and A_4 are absorption dips that become the most pronounced at 488.0 nm. The sharp rise in the PL at energies close to 1.6 eV arise from the GaAs substrate. The arrow identifies the Raman peak related to an impurity.

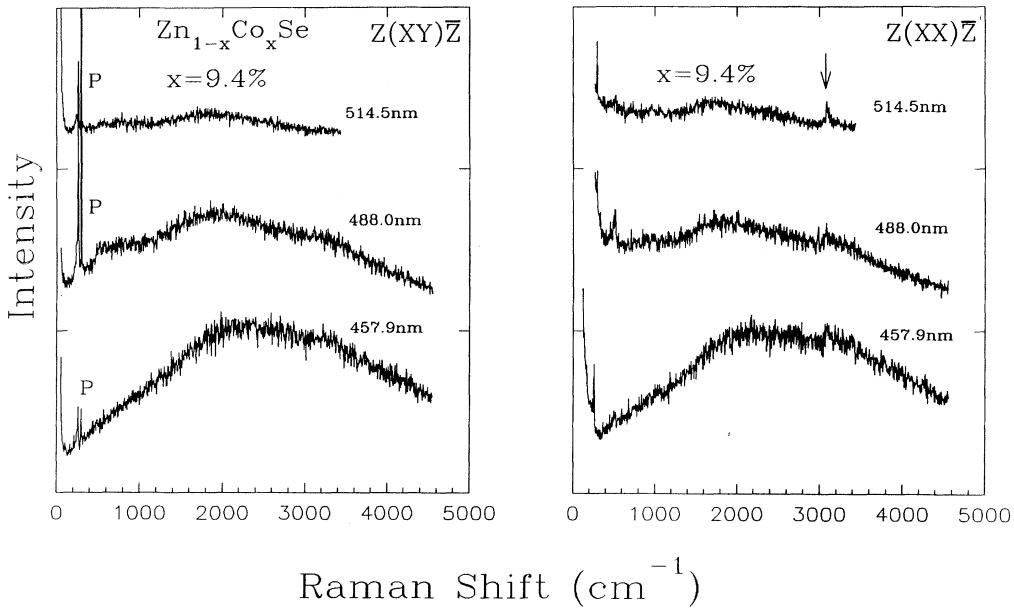

FIG. 3. Polarized $z(xx)\bar{z}$ and depolarized $z(xy)\bar{z}$ Raman spectra recorded with three different excitation wavelengths at 10 K from $Zn_{1-x}Co_xSe$ ($x=0.094$) showing resonant behavior of the Raman continuum. The arrow identifies the Raman peak related to the same impurity as in Figs. 1 and 2.

position (~ 2000 cm^{-1}), its width and appearance only when the PL associated with the $3d$ ions begin to broaden. The most striking difference between the continuum in the two series of samples is that it turns on only at a much higher Fe concentration ($x \sim 0.3$) in comparison to that in the case of Co ($x \sim 0.03$) doping.

IV. DISCUSSION

A. Luminescence: $Zn_{1-x}Co_xSe$ and $Zn_{1-x}Fe_xSe$

The luminescence bands in undoped ZnSe are similar to those previously reported.[15,16] The peaks at 2.24 (SA_1), 2.09 (SA_2), and 1.92 eV (SA_3) are self-activated (SA) emission bands from zinc vacancies and impurities in the ZnSe lattice.[15] S_0 and S_1 are related to donor-acceptor pair recombinations involving shallow donors and deep traps.[16] The Y transition has been associated with electronic states on dislocations while Y-LO is the optical-phonon replica of this peak.[16] As the Co concentration increases to 0.76% the PL bands of ZnSe are quenched. This suggests that in addition to substituting for Zn the Co ions fill Zn vacancies. A similar conclusion is applicable to the Fe-doped ZnSe samples. The 3100-cm^{-1} Raman peak, observed in all samples including undoped ZnSe, is impurity related; a possibility is chlorine.

In order to identify the origin of PL bands I, II, and III in $Zn_{1-x}Co_xSe$ and emission in $Zn_{1-x}Fe_xSe$, the relevant multiplet energy structure of Co^{2+} and Fe^{2+} in ZnSe are reproduced in Figs. 5(a) and 5(b) from Ref. 17. While electric dipole transitions between states constructed of pure d functions are forbidden, spin-orbit interaction and lack of inversion symmetry in the zinc-blende structure, however, allow such transitions. The observed transitions in $Zn_{1-x}Co_xSe$ are identified by arrows in Fig. 5(a) where the numbers I, II, and III correspond to the transitions yielding bands I, II, and III in Fig. 1. The label A in Fig. 5(a) relates to the absorption dips evident in Fig. 2.

We identify the transition $^2T_1 \rightarrow {}^4A_2$ with the narrow emission peak L. The initial state associated with L has been previously associated as either the $^2T_1$ excited multiplet level of the Co^{2+} ion,[18] or the exciton state $[Co^{3+}\cdot e]$.[14] Our recent high-pressure measurements[19] confirm that the energy of peak L decreases with pressure at a rate (~ 1.4 cm^{-1}/ K bar) in contrast to the increase of ~ 56 cm^{-1}/K bar pressure dependence of the ZnSe band gap.[20] Hence this would make the excitonic state unlikely to be associated with L. Moreover, if the exciton model is applicable, then the exciton binding energy of ~ 200 meV (see below) will not account for the quenching of L we observe at temperatures greater than 200 K.

We assign luminescence II and III as transitions from $^2T_1$ that terminate at the intermediate spin-quartet excited states of Co^{2+}, i.e., $^2T_1 \rightarrow {}^4T_2(F)$ and $^2T_1 \rightarrow {}^4T_1(F)$, respectively. The spectral line width of bands I and II differ significantly. Within the crystal-field approximation, transition energies between levels of the same electron configurations (same m and n in an $e^m t^n$ configuration) are independent of pressure and fluctuations of the cubic field arising from nuclear relaxation. Transitions between different configurations, however, are broadened due to fluctuations.[21] This is consistent with our assignment of the initial state ($^2T_1$) to an e^4t^3 configuration. In this case L is narrow since the final state $^4A_2$, characterized by an e^4t^3 configuration, does not involve changes in m and n. In contrast, luminescence II is broad since the final state $^4T_2(F)$ is characterized by e^3t^4 configuration. The transition associated with

PL III, $^2T_1 \rightarrow {}^4T_1(F)$, should be weak since optical transitions are forbidden between $e^n t^m$ and $e^{n+k} t^{m-k}$ levels for $|k| \geq 2$.[21] It is likely that this transition is observed due to configuration mixing,[21] i.e., an admixture of $^4T_1(F)$ with either an e^3t^4 or an e^4t^3 level.

From Fig. 5(b), we assign the 1.89-eV PL peak in $Zn_{1-x}Fe_xSe$ to connect the $^3A_2 \rightarrow {}^5E$ transition. The ^5E and $^3A_2$ states have configurations e^3t^3 and e^2t^4, respectively, and thus the luminescence is expected to be broad since the transition connects levels with different electron configurations. The observed 70-meV width of this transition is comparable to the 60-meV line width of the $^2T_1 \rightarrow {}^4T_1$ transition in $Zn_{1-x}Co_xSe$. This assignment of the optical transition in $Zn_{1-x}Fe_xSe$ is consistent with the absorption data of ZnS:Fe,[22] where the oscillator strength is strongest for the $^5E \rightarrow {}^3A_2$ transition compared to other spin-forbidden transitions. The transition $^3A_2 \rightarrow {}^5T_2$ [Fig. 5(b)] occurs at 1.50 eV and therefore overlaps with the emission from the GaAs substrate.

On the left-hand side of the energy axis of Fig. 5(c) we schematically represent the ZnSe valence separated by 2.8 eV from the conduction bands (CB). The valence bands arise predominantly from the hybridization of Zn 3*d* orbitals and Se 4*p* orbitals. In general it is not obvious

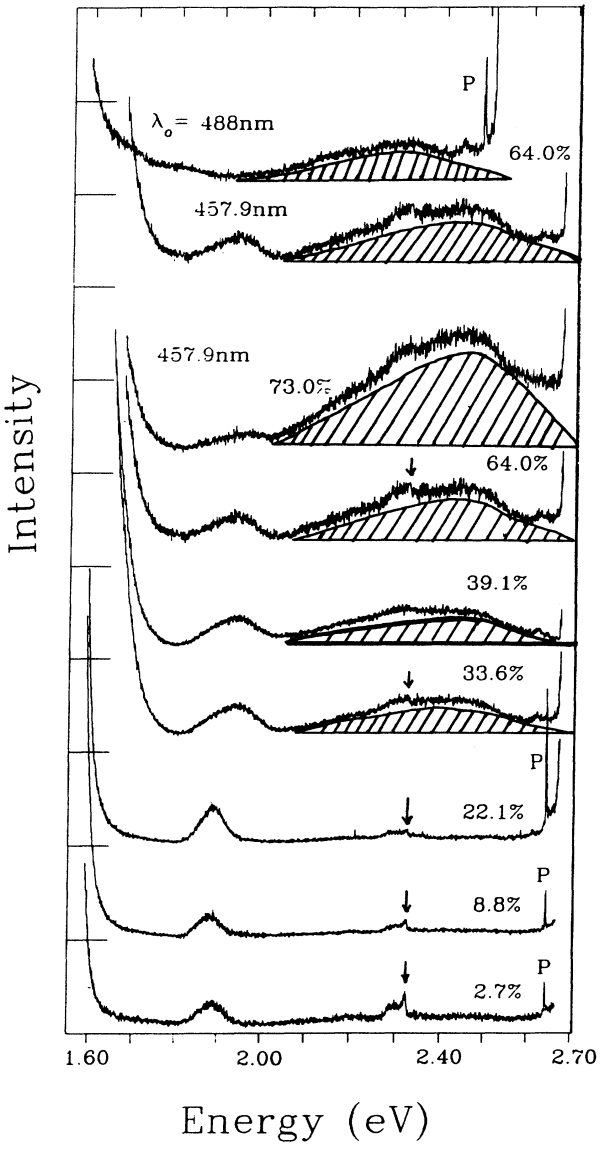

FIG. 4. Photoluminescence (PL) and Raman spectra at 10 K from several $Zn_{1-x}Fe_xSe$ films for $0.027 < x < 0.75$. All spectra, except the top one, were recorded with 457.9 nm excitation wavelength. The peak around 1.9 eV is PL. The hatched regions for $x > 0.33$ highlight the continuum of Raman excitations, while the sharp peaks *P* are Raman phonons. The peak identified by an arrow is extrinsic as in $Zn_{1-x}Co_xSe$ (Fig. 1). All spectra have been normalized to account for the different film thicknesses.

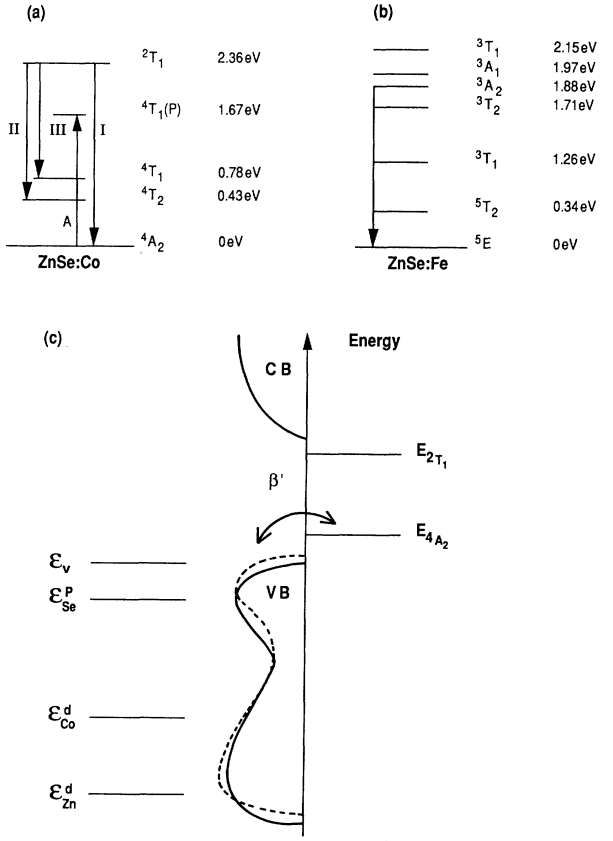

FIG. 5. (a) Crystal-field split manifold of Co^{2+} in ZnSe from Ref. 17 (spin-orbit effects hve not been included). Transitions I, II, and III relate to the photoluminescence bands shown in Fig. 1, while *A* is related to the dips A_1, A_2, A_3, and A_4 of Fig. 2 arising from spin-orbit splitting of the $^4T_1(P)$ state. (b) Crystal-field split manifold of Fe^{2+} in ZnSe from Ref. 17. The transition identified relates to the photoluminescence at ~1.9 eV in Fig. 4. (c) To the left of the energy axis we schematically represent the one-electron conduction and valence bands (solid line) in ZnSe. The one-electron energies ε^d_{Zn}, ε^d_{Co}, and ε^p_{Se} are the Zn-*d*, Co-*d*, and Se-*p* one-electron levels, respectively, and ε_v is the valence-band maximum. The dashed line is the slightly shifted valence band due to the replacement of Zn by Co. As in (a) the $^2T_1$ and $^4A_2$ states are discrete many-body levels. The effective exchange β' couples the host with the impurity.

how to place the many-electron atomic levels shown in Figs. 5(a) and 5(b) with respect to the one-electron valence-band maximum, ε_v. However, from electroabsorption[23] (EA) and photoluminescence excitation (PLE) data,[14] the ground state ($^4A_2$) of Co^{2+} is known to lie ~ 2.56 eV below the conduction band. Since L occurs at 2.361 eV, it follows that the initial state associated with this optical transition is ~ 200 meV below the conduction band.

We propose that the very rapid broadening of PL emissions I and II for Co concentrations beyond 1.6% reflects the proximity of the lowest Co configuration to the valence-band maximum. We denote the quantity which determines to what extent valence-band states mix into the localized levels as β', which can also be viewed as the rate at which electrons hop from and to the ground state of the impurity site into the valence band. So the effective exchange interaction, β' has the form

$$\beta'(x) \sim (V_{p^4A_2})^2 \times \frac{1}{E_{^4A_2} - \epsilon_v(x)} .$$

While this equation is similar to the equation for the one-electron *pd* hybridization, β, in the more familiar case of Mn in CdTe (see Ref. 24) there are some important differences:

(i) $V_{p^4A_2}$ represents the hopping of an electron out of the $^4A_2$ impurity many-electron ground state into the valence band rather than the one-electron hopping, V_{pd}, which essentially determines the valence-band width.

(ii) We have neglected, as small, the term where the intermediate state would be a d^8 state which lies higher in energy by about $U \sim 2.5$ eV (Ref. 23) (the effective intrasite Coulomb energy).

(iii) The denominator is the difference of a many-electron term and an one-electron term. While this normally implies the neglect of relaxation effects in the many-body state, that is not the case here. The $^4A_2$ level was positioned relative to the conduction-band minimum by comparison to PLE and EA experiments[14,23] and so these relaxation effects are already implicitly included in the $^4A_2$ level position.

It is well known from rare-earth and actinide physics that if the fluctuation rate becomes too large, the impurity level very rapidly loses its localized nature and becomes extended.[25,26] Analogously we expect the extent of delocalization of the many-electron state of Co-impurity atoms to be very sensitive to β'. While there are many reasons why β' could depend on x, we propose that the dependence comes predominantly from an upwards shift in the valence-band maximum on doping, i.e., the replacement of Zn by Co introduces a dependence of ε_v on x.

While a theoretical treatment of the shifts of the valence-band edge for $Zn_{1-x}Co_xSe$ does not exist, an analysis for $Cd_{1-x}Mn_xTe$ shows that the valence-band maximum increases steadily by about 0.5 eV as the Mn concentration increases from zero to 60%.[27] This dependence (~ 1 eV per Cd atom replaced by Mn) is rather weak. However, on alloying Co into ZnSe, we expect a larger shift as the *one-electron* Co-*d* levels, ε^d_{Co}, lie higher above *one-electron* Zn levels, ε^d_{Zn}, than does the majority Mn levels. (We also point out that as well as the upwards shift, one should expect a broadening of the valence-band states due to extra scattering from the random potential. This can also be viewed as an upwards shift of the "effective" valence-band maximum, and indeed might well dominate the shift in the case of 30% Fe substitution.) Since the locations of many-body crystal-field split Co *d* levels are, to a good approximation, independent of x and the spacing ($E_{^4A_2} - \varepsilon_v$) at $x < 0.01$ is only 0.25 eV, the valence-band edge will approach the low-lying $^4A_2$ state as x increases. It thus follows that β' will increase rapidly with increasing Co concentration. These effects are not seen in Mn-doped systems, where ($E_{^6A_1} - \varepsilon_v$) ~ -2 eV (Ref. 28) and therefore the effect of shifting ε_v is very small. On the other hand, as the Fe^{2+} ground state ^5E initially lies over 1 eV from the valence-band edge,[29] the same effect is seen. But, a larger doping concentration will be required prior to the occurrence of significant enhancement in the effective exchange interaction in these alloys. Moreover, very recent PL measurements from two (ZnCo)Se films[19] under hydrostatic pressure are also consistent with the broadening of the ground $^4A_2$ level arising from direct enhancements in β' through pressure.

These concentration dependencies of β' are consistent with the observed broadening of the PL transitions involving the low-lying *d* levels in the two alloys. At a given Co concentration the exchange interaction will be greatest for the $^4A_2$ ground state with the exchange decreasing progressively for the higher-lying $^4T_1$ and $^4T_1$ Co *d* levels. This level interaction hence gives rise to the broadening and eventual weakening of the PL associated with transitions connecting to the $^4A_2$ state in the optical emission. At $x = 0.037$ and beyond PL bands I and II both appear to have been quenched. This would argue for the ground state as well as the first excited state $^4T_2$ being broadened through exchange at this concentration. On the other hand, it is evident from Fig. 1 that PL III [$^2T_1 \rightarrow {}^4T_1(F)$] remains well defined until x approaches 9.4%, the highest Co concentration used in this study. This is consistent with the location of the final state ($^4T_1$) being initially over 1 eV from the valence-band edge and therefore a higher Co concentration is required prior to being broadened through the *p-d* exchange.

Since the strength of the nearest-neighbor Co^{2+}-Co^{2+} and Fe^{2+}-Fe^{2+} exchange integrals, J^{Co}_{dd} and J^{Fe}_{dd} can be viewed as a superexchange involving *p-d* hybridization,[30] we expect the *d-d* coupling to also increase with x. The fact that $J^{Co}_{dd} > J^{Fe}_{dd}$ (Ref. 31) is also in agreement with delocalization and band formation occurring at lower dopant concentration in $Zn_{1-x}Co_xSe$ than in $Zn_{1-x}Fe_xSe$.

We now briefly digress to understand why PL bands I, II, and III are strongest for excitation at 457.9 nm (2.7 eV) and to account for the absorption dips shown in Fig. 2. We note that the Co^+ acceptor state lies very close to the Co^{2+} excited state $^2T_1$. This is consistent with previous estimates of the location of the Co acceptor level in ZnSe that lies about 2.7 eV from the valence-band max-

imum.[23] Upon exciting at 457.9 nm, an electron from the valence band resonantly excites a Co^{2+} ion to the Co^{+} state. This Co^{+} state then relaxes nonradiatively to the neighboring $^2T_1$ state prior to radiative recombination at the low-lying $^4A_2$, $^4T_2$, and $^4T_1$ Co levels.

The rise in the luminescence at ~ 1.6 eV in Figs. 1 and 2 arises from emission associated with the substrate (GaAs). This contribution is strongest in the 1.6% film for excitation at 488.0 nm due to weak absorption in the (ZnCo)Se epilayer and the relatively small thickness of this film. The dips (A_1-A_4) in the luminescence spectra (Fig. 2) in this spectral region are assigned to $^4A_2 \rightarrow {}^4T_1(P)$ absorption transitions in the (ZnCo)Se layer of photons originating as PL from the substrate. The occurrence of four absorption dips (A_1-A_4) is likely due to spin-orbit splitting of the $^4T_1(P)$ state. The latter interaction splits the $^4T_1(P)$ state into four levels Γ_6 (A_4), Γ_8 (A_3), Γ_7 (A_2), and Γ_8 (A_1).[32]

B. Raman continuum

The study of electronic excitations in semiconductors by Raman scattering has received much attention.[33,34] These studies have largely focused on the case of excitations of shallow levels. Generally excluded in these discussions is the class of deep-level electronic transitions associated, as in the present study, with transition-metal atoms in semiconductors. The samples utilized in our work differ from shallow impurity-doped semiconductors in several important aspects; these differences have been discussed in the Introduction. We note that in spite of the high concentration of randomly distributed magnetic ions and the resulting structural disorder, standard ideas of semiconductor physics, i.e., energy gaps, effective masses, etc., are found to remain valid in the Co- and Fe-based DMS.[5,35]

We identify the broad polarized and depolarized Raman peaks evident in Figs. 1 and 3 to be associated with electronic excitations within the broadened crystal-field split $3d$ manifold. As discussed above, broadening of the crystal-field levels with increasing x in the alloy primarily occurs through enhanced exchange with the band electrons as well as contributions from the d-d interaction.[36] As seen from Fig. 5, at low Co and Fe concentrations the separations between the first few low-lying crystal-field states of Co^{2+} and Fe^{2+} are about 0.35 eV. Thus as these levels broaden and overlap, one expects that the resulting band will be a few tenths of an electron volt wide. The Raman continuum observed in both alloys does extend to 4000 cm^{-1} (0.5 eV) and is thus in agreement with our assertion that the inelastic scattering events occur within the strongly hybridized d levels. The enhancement of the Raman continuum in Fig. 3 for $\lambda_0=457.9$ nm is due to the near resonance of the exciting radiation with the transition connecting the ground state of Co^{2+} ($^4A_2$) to the bottom of the conduction band.

Our identification of the nature of the continuum is also consistent with the following findings. (1) As shown in Fig. 1, the continuum appears only in $Zn_{1-x}Co_xSe$ samples with $x>0.03$ when the discrete PL bands broaden; i.e., only when the electronic levels associated with Co^{2+} become more delocalized due to p-d coupling with the band electrons. (2) It is found that the continuum in $Zn_{1-x}Co_xSe$ appears at a critical concentration ($x\sim 0.03$) that is much smaller than the critical Fe concentration ($x\sim 0.33$) needed for the onset of the continuum in $Zn_{1-x}Fe_xSe$ (see Fig. 4). These differences of the continuum in $Zn_{1-x}Co_xSe$ and $Zn_{1-x}Fe_xSe$ are related, as discussed in the previous section, to the distinct dependencies of β' on x in the two alloys. (3) We eliminate dopant-induced structural disorder as the source of the Raman continuum in $Zn_{1-x}Co_xSe$ for $x>0.03$, since the continuum is *not* observed in $Zn_{1-x}Fe_xSe$ at similar Fe concentrations where the same degree of disorder would be present. (4) Since the continuum has comparable intensity at 300 and 5 K, it is not related to higher-order phonon or magnetic excitations, while the possibility of a broad plasmon excitation is ruled out since the samples are insulting. (5) Recent high-pressure measurements[19] show that it is possible to tune in coupling between the zone center LO phonon and the Raman continuum in $Zn_{1-x}Co_xSe$ samples below the critical Co concentration ($x\sim 0.03$) where there is no continuum at ambient pressures. This tunability is consistent with a pressure-enhanced exchange of the $3d$ electronic levels giving rise to the Raman continuum. We thus conclude that the continuum observed in $Zn_{1-x}Co_xSe$ ($Zn_{1-x}Fe_xSe$) for $x>0.03$ ($x>0.3$) is electronic in origin and arises from excitations within the hybridized crystal-field levels.

We now briefly address the issue of the insulating nature of all samples investigated in this study and its relation to the Raman continuum observed beyond critical Co and Fe concentrations. The optical measurements presented above reveal delocalization of $3d$ electrons at sufficient doping when p-d and d-d exchange are strong. At the high level of doping required in these systems, disorder must be taken into account.

In disordered systems a metal to insulator transition may occur due to electronic levels at the Fermi energy becoming localized as described by the Anderson Hamiltonian.[37] In this model randomness is introduced by having the on-site energies vary independently from site to site. For a given electron density the transition from metal to insulator occurs when the ratio of the random energy spread W to the hopping term t ($\sim V_{pd}^2$) exceeds a critical value. A metal-insulator transition can also result from electron-electron interactions. In the Hubbard model[38] when U, the onsite Coulomb energy, is large compared to t the band splits into two subbands with a gap between them. If there is one electron per site, the lower subbands for both spins will be full and upper ones empty, and the system will be an insulator. Both models of the transition to an insulating state are favored by a small hopping term. The combined effects of disorder and onsite repulsion on the metal to insulator transition are, however, not fully understood. Nevertheless, one would expect that the introduction of disorder in the Hubbard model causes subbands to broaden and overlap if the gap is small; thus the Hubbard transition to the metallic phase will be suppressed by the disorder. Our optical measurements are consistent with such disorder and the large U leading to the continuum of *localized* elec-

tronic states in the more heavily doped $Zn_{1-x}Co_xSe$ and $Zn_{1-x}Fe_xSe$ films.

V. CONCLUSIONS

In summary we have reported on the photoluminescence and Raman excitations associated with *deep* 3*d* levels in $Zn_{1-x}Co_xSe$ and $Zn_{1-x}Fe_xSe$. These systems are therefore distinct from the situation of shallow impurities in semiconductors where the relevant impurity interactions occur on the scale of the *s*-electron Bohr radius which is much larger than the lattice constant. Several optical transitions within the crystal-field split manifold are identified that broaden and weaken as x increases beyond a critical concentration of about 3% (Co) and 33% (Fe). It is proposed that an increase in the exchange between the *d* levels and band electrons with concentration x accounts for the broadening of the ground and lower excited crystal-field split *d* levels leading to dramatic changes in the optical emission. Beyond the critical concentration, a broad Raman continuum associated with scattering within the hybridized 3*d* levels is observed in both alloys. This result is in agreement with the proposed increased effective exchange interaction leading to band formation. The roles of correlations and disorder arising from the randomness of the dopant distribution in accounting for the Raman continuum and the insulating nature of the samples have also been discussed.

ACKNOWLEDGMENTS

We acknowledge that useful correspondence with Dr. K. Hass. Work at the Ohio State University was supported by the National Science Foundation under Contract No. DMR 90-01647 and that at NRL by the Office of Naval Research. Partial Support for M.M.S. was provided by the Department of Energy (DOE)–Basic Energy Sciences, Division of Material Sciences.

[1]G. A. Thomas, M. Capizzi, F. DeRosa, R. N. Bhatt, and T. M. Rice, Phys. Rev. B **23**, 5472 (1981).

[2]P. J. Colwell and M. V. Klein, Phys. Rev. B **6**, 498 (1972).

[3]M. Chandrasekhar and M. Cardona, Phys. Rev. B **16**, 3579 (1977).

[4]M. Chandrasekhar, J. B. Renucci, and M. Cardona, Phys. Rev. B **17**, 1623 (1978).

[5]*Diluted Magnetic Semiconductors,* edited by J. K. Furdyna and J. Kossut, Semiconductors and Semimetals, edited by R. K.Willardson and A. C. Beer (Academic, San Diego, 1988), Vol. 25.

[6]J. K. Furdyna, J. Appl. Phys **64**, R29 (1988).

[7]J. P. Lascaray, J. Diouri, M. El Amrani, and D. Coquillat, Solid State Commun. **47**, 709 (1983); Y. R. Lee, A. K. Ramdas, and R. L. Aggarwal, Phys. Rev. B **38**, 10 600 (1988).

[8]J. E. Morales Toro, W. M. Becker, B. I. Wang, U. Debska, and J. W. Richardson, Solid State Commun. **52**, 41 (1984).

[9]J. E. Morales Toro, W. M. Becker, B. I. Wang, and U. Debska, Phys. Rev. B **40**, 1186 (1989); A. K. Arora, E.-K. Suh, U. Debska, and A. K. Ramdas, *ibid.* **37**, 2927 (1988).

[10]A. Anastassiadou, E. Liarokapis, and E. Anastassakis, Phys. Scr. **38**, 444 (1988).

[11]*Growth, Characterization and Properties of Ultrathin Magnetic Films and Multilayers,* edited by B. T. Jonker, E. E. Marinero, and J. P. Heremans, Materials Research Society Symposia Proceedings No. 151 (MRS, Pittsburgh, 1989).

[12]X. Liu, A. Petrou, B. T. Jonker, G. A. Prinz, J. J. Kerbs, and J. Warnock, Appl. Phys. Lett. **55**, 1023 (1989); T. M. Giebultowicz, P. Klosowski, J. J. Rhyne, T. J. Udovic, J. K. Furdyna, and W. Giriat, Phys. Rev. B **41**, 504 (1990); J. P. Lascaray, F. Hamdani, D. Coquillat, and A. K. Bhattacharjee, J. Magn. Magn. Mater **104-107**, 995 (1992); A. Lewicki, A. I. Schindler, P. M. Shand, B. C. Crooker, and J. K. Furdyna, Phys. Rev. B **44**, 6137 (1991).

[13]B. T. Jonker, S. B. Qadri, J. J. Kerbs, and G. A. Prinz, J. Vac. Sci. Technol. A **6**, 1946 (1988); B. T. Jonker, S. B. Qadri, J. J. Kerbs, G. A. Prinz, and L. Salamanca-Young, *ibid.* **7**, 1360 (1989).

[14]D. J. Robbins, P. J. Deans, C. L. West, and W. Hayes, Philos. Trans. R. Soc. London, Ser. A **304**, 499 (1982); D. J. Robbins, J. Lumin. **24&25**, 137 (1981).

[15]J. C. Bouley, P. Blanconnier, A. Herman, Ph. Ged, P. Henoc, and J. P. Noblanc, J. Appl. Phys. **46**, 3549 (1975).

[16]P. J. Dean, Phys. Status Solidi A **81**, 625 (1984).

[17]A. Fazzio, M. J. Caldas, and A. Zunger, Phys. Rev. B **30**, 3430 (1984). Electronic levels of Co^{2+} and Fe^{2+} in DMS's are also discussed in M. Villeret, S. Rodriguez, and E. Kartheuser, Physica B **162**, 89 (1990).

[18]J. M. Noras, H. R. Szawelska, and J. W. Allen, J. Phys. C **14**, 3255 (1981); E. M. Wray and J. W. Allen, *ibid.* **4**, 512 (1971).

[19]U. D. Venkateswaran, C. L. Mak, R. Sooryakumar, and B. T. Jonker, Bull. Am. Phys. Soc. **38**, 797 (1993); C. L. Mak, U. D. Venkateswaran, R. Sooryakumar, and B. T. Jonker (unpublished).

[20]P. Jaszczyn-Kopec, B. Canny, G. Syfosse, and H. Hammel, Solid State Commun. **49**, 795 (1984).

[21]S. Sugano, Y. Tanabe, and H. Kamimura, in *Multiplets of Transition-Metal Ions in Crystals,* edited by H. S. W. Massey and K. A. Brueckner, Pure and Applied Physics (Academic, New York, 1970), Vol. 33.

[22]M. Skowronski and Z. Liro, J. Phys. C **15**, 137 (1982).

[23]V. I. Sokolov, T. P. Surkova, M. P. Kulakov, and A. V. Fadeev, Phys. Status Solidi B **130**, 267 (1985); V. I. Sokolov, A. N. Mamedov, T. P. Surkova, M. V. Chukichev, and M. P. Kulakov, Opt. Spektrosk. **62**, 805 (1987) [Opt. Spectrosc. (USSR) **62**, 480 (1987)]; T. Dietl, in *Semimagnetic Semiconductors and Diluted Magnetic Semiconductors,* edited by M. Averous, and M. Balkanski (Plenum, New York, 1991).

[24]A. K. Bhattacharjee, G. Fishman, and B. Coqblin, Physica B **117&118**, 449 (1983); B. E. Larson, K. C. Hass, and H. Ehrenreich, Phys. Rev. B **37**, 4137 (1988).

[25]For example, the low-temperature specific heat of $UAs_{1-x}Sb_x$ is found to be extremely sensitive to subtle changes in the 5*f*-conduction-band hybridization, see H. Rudigier, H. R. Ott, and O. Vogt, J. Magn. Magn. Mater. **63&64**, 159 (1987). Also J. M. Imer, D. Malterre, M. Grioni, P. Weibel, B. Dardel,and Y. Baer, Phys. Rev. B **44**, 10 455 (1991), showed that the change in hybridization on going from UPt_3 to UPd_3 dramatically affects the XPS spectrum.

[26]B. R. Cooper, R. Siemann, D. Yang, P.Thayamballi, and A. Banerjea, in *Handbook on Physics and Chemistry of the Actinides,* edited by A. J. Freeman and G. H. Lander (North-

Holland, Amsterdam, 1985), Vol. 2, Chap. 6, pp. 435–500.
[27]K. C. Hass and H. Ehrenreich, Physical Pol. A **73**, 933 (1988).
[28]V. I. Sokolov, A. N. Mamedov, V. V. Chernyaev, E. Z. Kurmaev, V. R. Galakhov, S. N. Nemnonov, M. P. Kulakov, and A. V. Fadeev, Fiz. Tverd. Tela (Leningrad) **27**, 2118 (1985) [Sov. Phys. Solid State **27** 1268 (1985)].
[29]K. P. O'Donnell, K. M. Lee, and G. D. Watkins, J. Phys. C **16**, 728 (1983).
[30]K. C. Hass, in *Semimagnetic Semiconductors and Diluted Magnetic Semiconductors,* edited by M. Averous and M. Balkanski (Plenum, New York, 1991).
[31]A. Twardowski, A. Lewicki, M. Arciszewska, W. J. M. de Jonge, H. J. M Swagten, and M. Demianiuk, Phys. Rev. B **38**, 10 749 (1988); A. Lewicki, A. I. Schindler, J. K. Furdyna, and W. Giriat, *ibid.* **40**, 2379 (1989).
[32]A. I. Ryskin, A. L. Natadze, and S. A. Kazanskiĭ, Zh. Eksp. Teor. Fiz. **64**, 910 (1973) [Sov. Phys. JETP **37**, 462 (1973)]; Herbert A. Weakliem, J. Chem. Phys. **36**, 2117 (1962).
[33]A. Pinczuk and E. Burstein, in *Light Scattering in Solid I,* edited by M. Cardona, Topics in Applied Physics (Springer, New York, 1975).
[34]M. V. Klein, in *Light Scattering in Solid I* (Ref. 33).
[35]B. T. Jonker, J. J. Kerbs, G. A. Prinz, X. Liu, A. Petrou, and L. Salamanca-Young, in *Growth, Characterization and Properties of Ultrathin Magnetic Films and Multilayers* (Ref. 11).
[36]J. B. Goodenough, in *New Developments in Semiconductors,* edited by P. R. Wallace, R. Harris, and M. J. Zuckerman (Noordhoff International, Leiden, 1973).
[37]P. W. Anderson, Phys. Rev. **109**, 1492 (1958).
[38]J. Hubbard, Proc. R. Soc. London Ser. A **276**, 238 (1963); **277**, 237 (1964); **281**, 401 (1964).